Scaling and Universality in Rock Fracture

Jörn Davidsen[*]

British Antarctic Survey, High Cross, Madingley Road, Cambridge CB3 0ET, United Kingdom

Sergei Stanchits and Georg Dresen

GeoForschungszentrumZentrum Potsdam, Department 3.2, Telegraphenberg D423, 14473 Potsdam, Germany

We present a detailed statistical analysis of acoustic emission time series from laboratory rock fracture obtained from different experiments on different materials including acoustic emission controlled triaxial fracture and punch-through tests. In all considered cases, the waiting time distribution can be described by a unique scaling function indicating its universality. This scaling function is even indistinguishable from that for earthquakes suggesting its general validity for fracture processes independent of time, space, and magnitude scales.

The fracture of materials is technologically of enormous interest due to its economic and human cost [1]. Despite the large amount of experimental data and the considerable efforts undertaken [2], many questions about fracture have not yet been answered. In particular, there is no comprehensive understanding of rupture phenomena but only a partial classification in restricted and relatively simple situations. For example, many material ruptures occur by a ''one crack'' mechanism and a lot of effort is being devoted to the understanding, detection, and prevention of the nucleation of the crack [3–8]. Exceptions to the one crack rupture mechanism are heterogeneous materials such as fiber composites, rocks, concrete under compression, and materials with large distributed residual stresses. In these systems, failure may occur as the culmination of a progressive damage involving complex interactions between multiple defects and microcracks.

In particular, acoustic emission (AE) due to microcrack growth precedes the macroscopic failure of rock samples under constant stress [9,10] or constant strain rate loading [11,12]. This is an example of the concept of ''multiple fracturing''—the coalescence of spontaneously occurring microcracks leading to a catastrophic failure—which is thought to be applicable to earthquakes as well despite the vastly different scales involved [13–15]. Because of this and the similarity in their statistical behavior, acoustic emissions can be considered analogous to earthquake sequences. The temporal [16,17], spatial [18], and size distribution [11] of AE events follow a power law, just as it is commonly observed for earthquakes [19,20]. Such power-law scaling can be considered indicative of self-similarity in the AE and earthquake source process [16].

The time evolution of AE and earthquake data also display considerable differences. Laboratory rock fracture is dominated by a large number of foreshocks while seismicity in the Earth's crust is characterized by an abundance of aftershocks [21]. Here, we show that despite this difference the probability density function (PDF) for the time interval between successive events is the same in both cases if they are rescaled with the mean waiting time or equivalently with the mean rate of occurrence. In particular, the PDF for laboratory rock fracture neither depends on the specific experiment nor on the specific material. These observations strongly suggest a universal character of the waiting time distribution and self-similarity over a wide range of activity in rock fracture.

In Ref. [22] it was shown that the PDF of earthquake waiting times—*without* distinguishing between foreshocks, main shocks, or aftershocks—for different spatial areas, time windows, and magnitude ranges can be described by a unique distribution if time is rescaled with the mean rate of seismic occurrence. It was shown, in particular, that the distribution holds from worldwide to local scales, for quite different tectonic environments, and for all magnitude ranges considered. This is even true if the seismic rate is not stationary as during periods of pronounced aftershock sequences when the rate decays according to Omori's law [23]. In those cases, the waiting times have to be rescaled by the instantaneous rate instead [22].

Here, we analyze in the same way the waiting times between AE events in time series of laboratory rock fracture obtained from different experiments. We initially restrict our analysis to periods of *stationary activity*, i.e., periods where pronounced activity peaks are absent and the mean rate of activity in any subperiod—the instantaneous rate—is statistically indistinguishable from the mean rate of the whole period. Yet, we will show below that this restriction can be relaxed as it is the case for earthquakes. Laboratory experiments were performed on five different materials: Flechtingen sandstone (Fb, porosity about 7%), Bleuerswiller sandstone (Vo, porosity 24%), Aue granite (Ag, porosity 1.3%), Tono granite (To, porosity 1.7%), and Etna Basalt (Eb, porosity 2.1%). Sandstone samples were fractured at wet condition (pore pressure 10 MPa), granite and basalt samples at dry conditions.

The formation of compaction bands was observed in the case of Vo sandstone [24] and brittle fracture in all other cases. We investigated the fracture of rock samples at confining pressures in the range 5–100 MPa in different axial loading conditions: constant displacement rate (CDR) of 20 μm/min, AE activity feedback control (AFC) of loading, as described in Ref. [25], and punch-through (PT) loading conditions [26]. The threshold level of the rate control sensor allowed varying the speed of the fault propagation by 3 orders of magnitude, i.e., from mm/s in CDR tests to μm/s in AE AFC tests. The newly developed data acquisition system (DaxBox made by PRÖKEL, Germany) records fully digitized waveforms (16 bit amplitude resolution, 10 MHz sampling rate) in 6 Gb memory buffer, providing zero dead time of registration (see [27] for a detailed discussion). Most importantly, the data acquisition system allows one to record AE events continuously even for high AE activity which is especially important for the analysis here. The only limitation on the shortest registered time intervals between subsequent AE events comes from the finite duration of the associated signals leading to the possibility of overlapping AE signals, for example, doublets or triplets. To simplify the fully automatic procedure of onset time picking and hypocenters location, only the first signal is located in a sliding window of 100 μs. Thus, the shortest time interval in the experiments considered here equals 100 μs, yet the onset times of AE arrivals at each particular channel were determined with accuracy of about 0.5 μs. For each experiment, we selected one or more periods of stationary activity for our analysis.

In the following, we focus on two quantities to characterize each AE event: time of occurrence and AE adjusted amplitude calculated according to the procedure described in Ref. [28]. While in most cases we consider all recorded AE events, we also study the effect of detection thresholds by only considering events with AE adjusted amplitude A above a certain threshold A_{th}. In both cases, the AE series is transformed into a point process where events occur at times t_i with $1 \leq i \leq N$, and therefore, the time between successive events can be obtained as $T_i = t_{i+1} - t_i$. These are the waiting times which are also referred to as recurrence times or interoccurrence times. For a given fracture experiment E, their PDF is denoted by $P_E(T)$.

Figure 1 shows the PDF of the normalized waiting times $\theta = T/\langle T \rangle$ for different rock fracture experiments where $\langle T \rangle$ is the respective mean waiting time. The excellent data collapse implies that $P(T/\langle T \rangle)$ does not depend on the particular rock fracture experiment and that we can write

$$P_E(T) = P(T/\langle T \rangle_E)/\langle T \rangle_E. \quad (1)$$

Thus for a given fracture experiment E, the PDF $P_E(T)$ of its AE series is determined by its mean waiting time $\langle T \rangle_E = (t_N - t_1)/(N - 1)$—or equivalently the mean rate $R_E = \langle T \rangle_E^{-1}$—and the universal scaling function $P(\theta)$
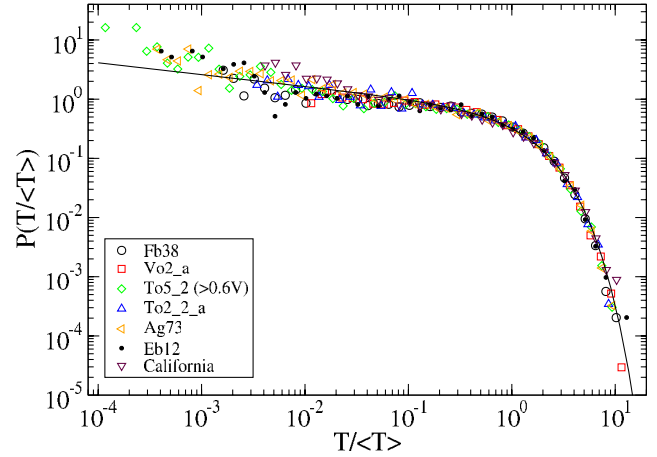

FIG. 1 (color online).   Probability density function of normalized waiting times $T/\langle T \rangle$ for five different rock fracture experiments (see Table I for details) and an earthquake catalog from southern California for comparison (see text for details). The solid line corresponds to a fit based on Eq. (2) with $\theta = T/\langle T \rangle$ giving $\gamma \approx 0.8$ and $B \approx 1.4$.

which can be well approximated by a gamma distribution

$$P(\theta) \propto \theta^{-(1-\gamma)} \exp(-\theta/B), \quad (2)$$

with $\gamma \approx 0.8$, $B \approx 1.4$ and the prefactor fixed by normalization [29]. Therefore, we have essentially a decreasing power law with exponent about 0.2, up to the largest values of the argument, $\theta = T/\langle T \rangle$ about 1, where the exponential factor comes into play. This is statistically indistinguishable (at the 2σ level) from the results for earthquake data given in Ref. [22], namely, $\gamma = 0.67 \pm 0.05$ and $B = 1.58 \pm 0.15$. As shown in Fig. 1, this is also confirmed by the PDF of an earthquake series from southern California which we have included for comparison [30].
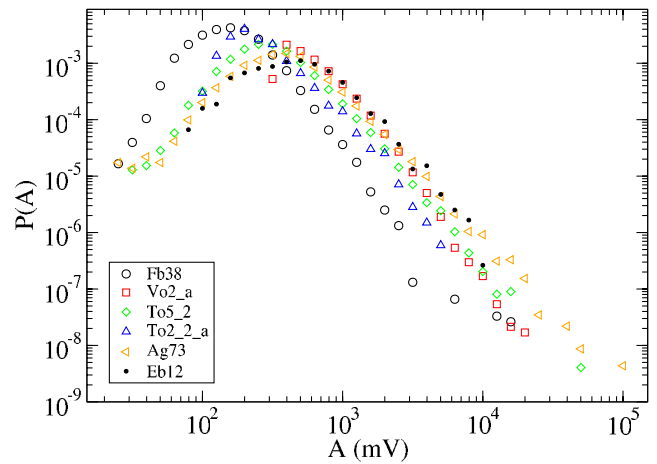

FIG. 2 (color online).   Probability density function of AE adjusted amplitude A for the same rock fracture experiments as in Fig. 1.
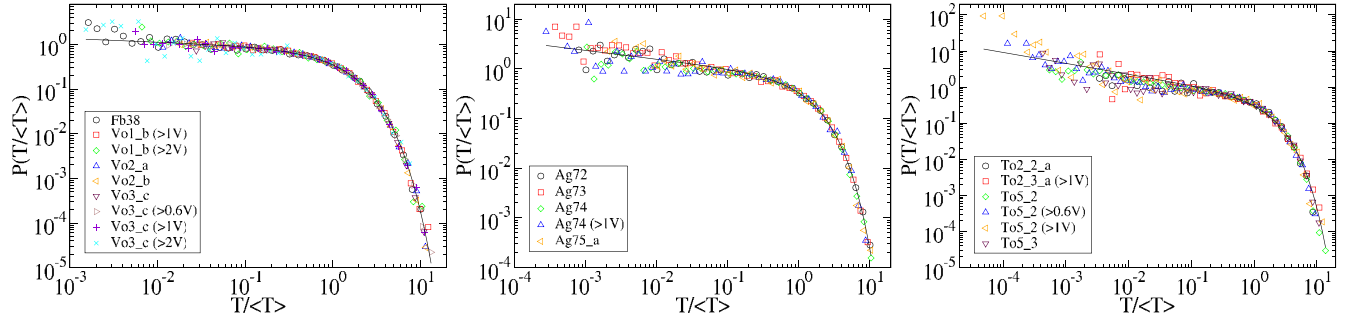
FIG. 3 (color online).   Probability density functions of normalized waiting times $T/\langle T\rangle$ for fracture experiments on sandstone, Aue granite, and Tono granite (from left to right); see Table I for details. The solid lines correspond to best fits according to Eq. (2) giving $\gamma = 0.92$ and $B = 1.2$, $\gamma = 0.82$ and $B = 1.3$, $\gamma = 0.70$ and $B = 1.5$, respectively.

In particular, $P(\theta)$ is independent of the frequency-amplitude distribution of the AE signal. As Fig. 2 shows, the PDF $P(A)$ for the AE adjusted amplitude A depends crucially on the particular experiment. While the overall structure of $P(A)$ is rather similar for the different experiments—a sharp increase up to a maximum value followed by a power-law–like decrease—details such as the location of the maximum and the slope β of the tail can be very different. For instance, the latter varies between 2.5 and 3.7 for the considered experiments. This corresponds to a variation in the Gutenberg-Richter exponent b between 1.1 and 1.9 which characterizes the frequency-magnitude relation of earthquakes [31,32]. Thus for our rock fracture experiments, the variation in b is larger than the regional variability in the earthquake data studied in [22]. Yet, $P(\theta)$ remains basically unchanged. More importantly, even considering only events above a lower threshold A_{th}, as for the data set To5_2 in Fig. 1, does not affect $P(\theta)$. This indicates the robustness of our results.

This robustness is further confirmed by Fig. 3, which shows $P(\theta)$ for a large selection of fracture experiments (see Table I for details). Again, $P(\theta)$ can be well described by Eq. (2). The slight variation in the fitted values of γ and B can be attributed mainly to statistical fluctuations and partially to measurement induced biases: The relatively high value of γ for sandstone is a consequence of the inability to detect the shortest waiting times due to measurement restrictions absent in the other experiments. This absence of short waiting times (an order of magnitude compared with granite) significantly biases the estimate of γ towards higher values.

Figure 3 shows not only that for sandstone and different types of granite the influence of the specific material on $P(\theta)$ is negligible but also that the type of experiment (punch through versus constant displacement rate versus activity feedback control) has no significant influence on $P(\theta)$. Moreover, Fig. 3 indicates that variations with A_{th} are negligible as well. Even restricting the included AE events to arbitrarily selected areas within the rock sample did not alter $P(\theta)$ (not shown). All these observations strongly

suggest that $P(\theta)$ given in Eq. (2) is a universal result for rock fracture. It further implies that $P(T)$ is self-similar over a wide range of activity rates spanning 2 orders of magnitude for the experiments considered here alone (see Table I).

Our results also indicate that the universal form of $P(\theta)$ can be recovered for AE signals with largely varying AE rates—as, for example, during periods of pronounced foreshock sequences—if instantaneous rates are used. As Table I shows, the AE signal of experiment Vo2 consists of at least two long periods of stationary activity, Vo2_a and Vo2_b, with different $\langle T\rangle$'s. Yet, the respective PDFs $P(\theta)$

TABLE I.   List of analyzed rock fracture experiments. Here, P_c is the confining pressure, A_{th} is the selected AE amplitude threshold, $\langle T\rangle$ is the mean waiting time, and N the number of AE events.

Name	Loading	P_c (MPa)	A_{th} (V)	$\langle T\rangle$ (sec)	N
FB38	AFC	50	0	0.0777	10 339
Vo1_b	CDR	100	1.0	0.0509	12 817
			2.0	0.189	3447
Vo2_a	CDR	60	0.0	0.110	12 708
Vo2_b	CDR	60	0.0	0.0687	26 218
Vo3_c	CDR	80	0.0	0.0453	30 287
			0.6	0.0943	14 564
			1.0	0.222	6188
			2.0	1.04	1318
Ag72	AFC	20	0.0	0.154	4465
Ag73	AFC	20	0.0	0.337	9860
Ag74	AFC	10	0.0	0.120	10 486
			1.0	0.453	2780
Ag75_a	AFC	20	0.0	0.0479	1838
To2_2_a	PT	5	0.0	0.0371	1445
To2_3_a	PT	30	1.0	0.0364	1700
To5_2	AFC	20	0.0	0.230	21 135
			0.6	1.07	4538
			1.0	2.58	1889
To5_3	AFC	30	0.0	0.369	2263
Eb12	AFC	20	0.0	0.776	1632

are indistinguishable as follows from Fig. 3. This implies that $P(\theta)$ for the combined signal is the same as well [33].

While we have presented strong evidence that $P(\theta)$ is universal for AE signals in rock fracture and earthquake sequences, the correlations between subsequent waiting times are very different. In Ref. [35], it was shown that the distribution of waiting times between earthquakes strongly depends on the previous waiting time, such that small and large waiting times tend to cluster in time. We find that this is not the case for the AE signals studied here. In contrast, the conditional PDF $P(\theta|\theta_0)$ is independent of the previous waiting time T_0 with $\theta_0 = T_0/\langle T \rangle$ and, thus, $P(\theta|\theta_0) = P(\theta)$. This might be due to the small number of pronounced foreshock and aftershock clusters of which the latter are particularly dominant in seismicity.

To summarize, we have shown that the probability density function for waiting times in laboratory rock fracture is self-similar with respect to the AE rate and can be described by a unique and universal scaling function $P(\theta)$. Its particular form can be well approximated by a gamma function implying a broad distribution of waiting times. This is very different from an exponential distribution expected for simple random Poisson processes and indicates the existence of a nontrivial universal mechanism in the AE generation process. The similarity with seismicity even suggests a connection with fracture phenomena at much larger scales and might help to understand this mechanism.

*Present address: Complexity Science Group, Department of Physics and Astronomy, University of Calgary, 2500 University Drive NW, Calgary, Alberta T2N 1N4, Canada. Electronic address: davidsen@pks.mpg.de

[1] D. Sornette, *Critical Phenomena in Natural Sciences* (Springer Verlag, Berlin, 2000).

[2] *Fracture*, edited by H. Liebowitz (Academic, New York, 1984), Vol. I–VII.

[3] K. J. Måløy, A. Hansen, E. L. Hinrichsen, and S. Roux, Phys. Rev. Lett. **68**, 213 (1992).

[4] M. Marder and J. Fineberg, Phys. Today **49**, No. 9, 24 (1996).

[5] P. Daguier, S. Henaux, E. Bouchaud, and F. Creuzet, Phys. Rev. E **53**, 5637 (1996).

[6] J. Fineberg and M. Marder, Phys. Rep. **313**, 1 (1999).

[7] M. J. Buehler and H. Gao, Nature (London) **439**, 307 (2006).

[8] K. J. Måløy, S. Santucci, J. Schmittbuhl, and R. Toussaint, Phys. Rev. Lett. **96**, 045501 (2006).

[9] D. Lockner and J. Byerlee, Bull. Seismol. Soc. Am. **67**, 247 (1977).

[10] T. Yanagidani, S. Ehara, O. Nishizawa, K. Kusunose, and M. Terada, J. Geophys. Res. **90**, 6840 (1985).

[11] K. Mogi, Bulletin of the Earthquake Research Institute, University of Tokyo **40**, 125 (1962).

[12] C. H. Scholz, J. Geophys. Res. **73**, 1417 (1968).

[13] D. L. Turcotte, *Fractals and Chaos in Geology and Geophysics* (Cambridge University, Cambridge, 1997), 2nd ed.

[14] C. H. Scholz, *The Mechanics of Earthquakes and Faulting* (Cambridge University, Cambridge, 2002), 2nd ed.

[15] N. M. Beeler, Pure Appl. Geophys. **161**, 1853 (2004).

[16] T. Hirata, J. Geophys. Res. **92**, 6215 (1987).

[17] I. O. Ojala, I. G. Main, and B. T. Ngwenya, Geophys. Res. Lett. **31**, 24 617 (2004).

[18] T. Hirata, T. Satoh, and K. Ito, Geophys. J. R. Astron. Soc. **90**, 369 (1987).

[19] C. Frohlich and S. D. Davis, J. Geophys. Res. **98**, 631 (1993).

[20] T. Utsu, Y. Ogata, and R. S. Matsu'ura, J. Phys. Earth **43**, 1 (1995).

[21] I. Main, Geophys. J. Int. **142**, 151 (2000).

[22] A. Corral, Phys. Rev. Lett. **92**, 108501 (2004).

[23] F. Omori, J. Coll. Sci., Imp. Univ. Tokyo **7**, 111 (1894).

[24] J. Fortin, S. Stanchits, G. Dresen, and Y. Gueguen, J. Geophys. Res. **111**, 10 203 (2006).

[25] A. Zang, F. C. Wagner, S. Stanchits, C. Janssen, and G. Dresen, J. Geophys. Res. **105**, 23 651 (2000).

[26] T. Backers, O. Stephansson, and E. Rybacki, Int. J. Rock Mech. Min. Sci. **39**, 755 (2002).

[27] S. Stanchits, S. Vinciguerra, and G. Dresen, Pure Appl. Geophys. **163**, 975 (2006).

[28] A. Zang, F. C. Wagner, S. Stanchits, G. Dresen, R. Andersen, and M. Haidekker, Geophys. J. Int. **135**, 1113 (1998).

[29] The deviations between the data and Eq. (2) for small arguments (see Fig. 1) are partially due to weak nonstationarities, namely, foreshock activity, and partially due to statistical uncertainties. The statistical uncertainties are especially pronounced for small arguments since the number of events in the corresponding bins is low.

[30] Data from http://www.data.scec.org/ftp/catalogs/SHLK/. We have considered all earthquakes within the rectangle $(118° \text{ W}, 115.0° \text{ W}) \times (32° \text{ N}, 35.0° \text{ N})$ from February 1995 until July 1997 and with magnitude larger than 2.0 giving $N = 2816$ and $\langle T \rangle = 7.70$ h.

[31] B. Gutenberg and C. Richter, *Seismicity of the Earth* (Princeton University, Princeton, NJ, 1949).

[32] We used $b = 1.44\frac{\beta-1}{2}$ which assumes $A^2 \propto E$ where E is the total energy of an AE event. In the case of earthquakes, E corresponds to the total energy in the seismic waves which can be related to the event's magnitude m by $\log_{10} E = 1.44 m + 5.24$ [13].

[33] If instantaneous rates are not used here, the nonstationarities lead to pronounced deviations at small and large arguments of $P(\theta)$. In particular, foreshock sequences with rate exponent p' will lead to a faster decay with an expected exponent $2 - 1/p'$ at short time scales similar to what has been observed for aftershock sequences in seismicity [22,34].

[34] R. Shcherbakov, G. Yakovlev, D. L. Turcotte, and J. B. Rundle, Phys. Rev. Lett. **95**, 218501 (2005).

[35] V. N. Livina, S. Havlin, and A. Bunde, Phys. Rev. Lett. **95**, 208501 (2005).